Lawrence Berkeley Laboratory

UNIVERSITY OF CALIFORNIA

Physics Division

Submitted to Physical Review Letters

SEARCH FOR RIGHT-HANDED CURRENTS USING MUON SPIN ROTATION

D.P. Stoker, B. Balke, J. Carr, G. Gidal, A. Jodidio, K.A. Shinsky, H.M. Steiner, M. Strovink, R.D. Tripp, B. Gobbi, and C.J. Oram

January 1985

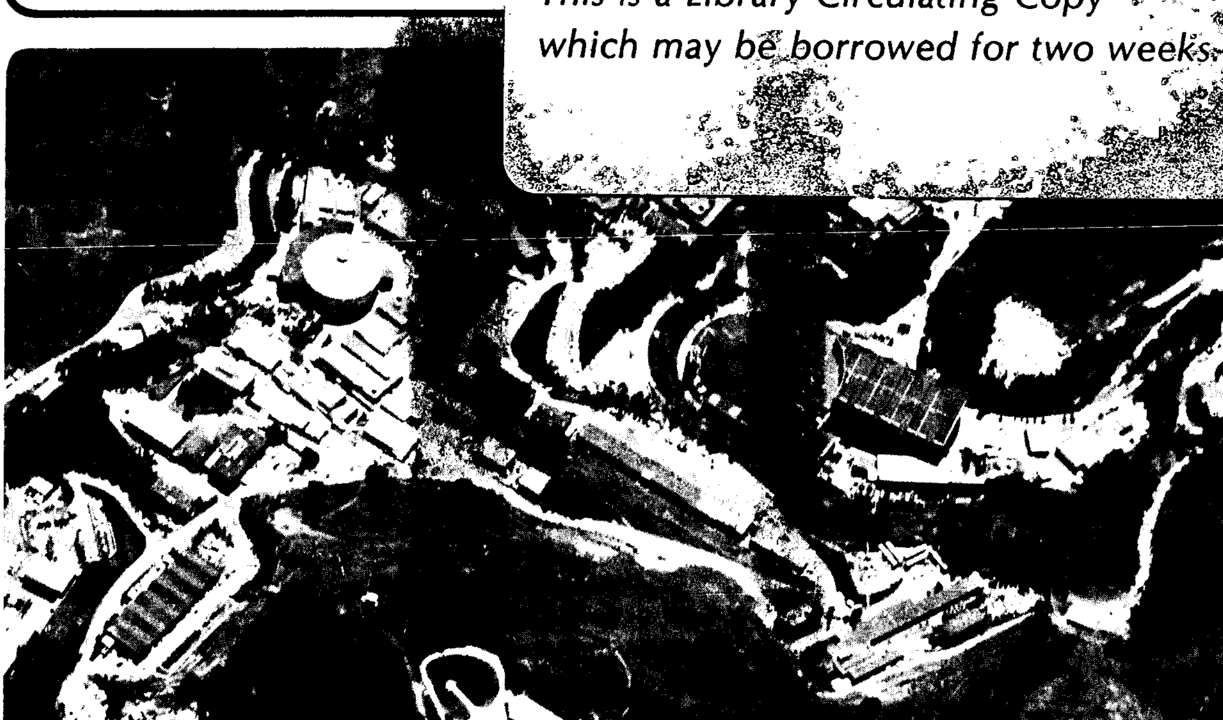

Prepared for the U.S. Department of Energy under Contract DE-AC03-76SF00098

DISCLAIMER

Search for Right-Handed Currents Using Muon Spin Rotation

D.P. Stoker, B. Balke, J. Carr[(a)], G. Gidal, A. Jodidio, K.A. Shinsky[(b)], H.M. Steiner, M. Strovink, and R.D. Tripp

Lawrence Berkeley Laboratory and Department of Physics, University of California, Berkeley, California 94720

and

B. Gobbi

Department of Physics, Northwestern University, Evanston, Illinois 60201

and

C.J. Oram

TRIUMF, Vancouver, British Columbia V6T 2A3, Canada

A μSR technique has been used to place limits on right-handed currents in μ^+ decay. The spins of polarized μ^+ stopped in metal targets were precessed by 70-G or 110-G transverse fields. The μSR signal amplitude produced by high momentum decay e^+ emitted near the beam direction implies $\xi P_\mu \delta/\rho > 0.9941$ and $M(W_2) > 350$ GeV (90% confidence), where W_2 is a predominantly right-handed gauge boson. The present result combined with our previous spin-held analysis yields $\xi P_\mu \delta/\rho > 0.9969$ and $M(W_2) > 410$ GeV.

In $SU(2)_L \times SU(2)_R \times U(1)$ left-right symmetric electroweak models[1] the charged gauge boson weak eigenstates (W_L, W_R) and mass eigenstates (W_1, W_2), are related by $W_1 = W_L\cos\zeta - W_R\sin\zeta$, $W_2 = W_L\sin\zeta + W_R\cos\zeta$. Stringent limits on the mixing angle ζ and the square of the mass ratio $\alpha = M^2(W_1)/M^2(W_2)$ are obtained from muon decay provided any ν_R that couples to W_R has negligible mass. We have previously reported limits[2] from an analysis of the e^+ momentum spectrum near the endpoint opposite to the μ^+ spin, where the V-A decay rate vanishes. Here we present additional limits based on a precise measurement of the decay e^+ spectrum asymmetry above 46 MeV/c using a muon spin rotation (μSR) technique.

The μSR data in Fig. 1 reflect the stopped μ^+ decay rate, relative to that for unpolarized muons,

$$R(\tilde{x},\theta) = 1 + \frac{1-2\tilde{x}}{1+2\tilde{x}} P_\mu A(\tilde{x})\cos\theta(t) \qquad (1)$$

where $\theta(t)$ is the angle between the direction of μ^+ polarization P_μ and the e^+ momentum direction $\hat{p}_e$, $\tilde{x} = 1-x=1-p_e/p_e(\max)$, and $A(\tilde{x})=\pm1$ in the $V\mp A$ limits. [Finite electron mass and radiative corrections[3] omitted from Eq. (1) are included in the analysis.] With the muon-decay parameters[3] ξ,δ, and ρ

$$A(\tilde{x}) \approx (\xi\delta/\rho)[1+2\tilde{x}(\frac{\tilde{\delta}}{1-2\tilde{x}} - \frac{3\tilde{\rho}}{1+2\tilde{x}})] \qquad (2)$$

where $\tilde{\delta}=1-4\delta/3$ and $\tilde{\rho}=1-4\rho/3$. In left-right symmetric theories[4] $P_\mu \approx 1-2(\alpha+\zeta)^2$ along $-\hat{p}_\mu$ for μ^+ from π^+ decay at rest. Normalized to that for V-A decay of μ^+ with $P_\mu = 1$, the μSR signal amplitude is $P_\mu A(\tilde{x})$, and the endpoint amplitude $P_\mu A(0) = \xi P_\mu \delta/\rho \approx 1-2(2\alpha^2+2\alpha\zeta+\zeta^2)$ restricts α and ζ.

The TRIUMF M13 beamline[5] produced an almost completely polarized 29.5 MeV/c beam of 15000 μ^+/sec within a 1% $\Delta p/p$ from π^+ decay at rest near the surface of the production target. A 2% admixture of prompt μ^+ from π^+ decay in flight was rejected by timing cuts with respect to the cyclotron rf cycle. The μ^+ beam entered the same apparatus that we have already described in detail[2], and came to rest in foils of ≥ 99.99% pure Al, Cu, Ag, and Au, or in liquid He. The μSR data were interleaved in hourly runs with spin-held data that formed the basis of our previously published analysis.[2] For μSR runs, the spin-holding longitudinal field

(B_L) at the target was nulled to within ± 2-G and instead a 70-G or 110-G transverse field (B_T) was applied. Decay e^+ emitted near the beam direction were focussed by a downstream solenoid into a cylindrical dipole spectrometer for momentum analysis. The stopped μ^+ and delayed e^+ provided the same trigger signature as described before. Here we present data from 3.7×10^7 triggers accumulated in three running periods spread over two years. Events with an extra beam particle arriving within ±10 μsec of the μ^+ stop were rejected, as were events with reconstructed μ^+-e^+ track separation >0.45 cm at the target, or polar angles $\cos\theta_\mu<0.99$ or $\cos\theta_e<0.975$. Additional cuts have been described previously[2].

As before, the decay e^+ momentum was obtained to first order from the sum of the horizontal coordinates at the conjugate foci of the spectrometer and its 1.07%/cm momentum dispersion. Empirical corrections, based on the μSR data endpoint, were made for deviation from the median plane and according to impact parameter with respect to the magnet axis. The resulting momentum resolution is better than 0.2% rms. The spectrometer momentum scale was calibrated with e^+ beams obtained at several settings of the NMR-monitored beamline elements. A consistent independent calibration was determined from the μSR data endpoint positions in runs using different spectrometer settings. Events with $x<0.88$, having lower statistical power and larger uncertainties in x, were rejected. After all cuts 5.6% of the μSR raw triggers were retained.

The μSR data in six 0.02 wide x bins are fitted to

$$N(t) = N_0\left[\int C(x)dx + P_\mu A(\tilde{x})G(t)\langle\cos\theta\rangle_t \int D(x)dx\right]\exp(-t/\tau_\mu) \qquad (3)$$

We have checked that both the μSR and spin-held data are consistent with zero background. The fitted μ^+ mean life $\tau_\mu = 2.209 \pm 0.006$ (stat.) μsec, spin rotation frequency, and spin relaxation function G(t) representing the decay of the μSR signal seen in Fig. 1. are common to all x bins. C(x) and D(x) are the angle independent and dependent parts respectively of the radiatively corrected V-A differential decay rate, smeared by the e^+ energy-loss straggling and by a sum of Gaussian momentum resolution functions. Momentum acceptance corrections are made to C(x) and D(x) based on the measured and expected $\langle p_e \rangle$ within each x bin. The angular acceptance of the apparatus for decay e^+ is given by the $\hat{p}_e$ distribution observed in time-averaged isotropic μSR data. The corresponding parent μ^+ polarization directions $\hat{P}_\mu$, initially along $-\hat{p}_\mu$, precess with frequency $\omega \approx eB_T/m_\mu c$. With ω free in the fit, these $\hat{p}_e$ and precessing $\hat{P}_\mu$ distributions yield the $\langle \cos\theta \rangle_t$ appropriate to each 0.04 μsec time bin.

The decay of the μSR signal in Fig. 1 is due to loss of phase coherence between the precessing μ^+ spins. Fitting $P_\mu A(\tilde{x})G(t)$ to each spin precession cycle indicates approximately Gaussian spin relaxation functions G(t), as shown in Fig. 2. The fitted initial depolarization (12.4±0.9%) in liquid He may be due to μ^+-e^- spin exchange processes during μ^+ thermalization. In metals the high free electron concentration screens the μ^+ from interactions with individual electrons, but the μ^+ spins can be dephased by the local fields of randomly oriented nuclear magnetic dipole moments. In ideal metals the resulting spin relaxation for mobile μ^+, with mean lattice site residence time τ_c, is given approximately by the Kubo-Tomita expression[6] $\exp\{-2\sigma^2\tau_c^2[\exp(-t/\tau_c)-1+t/\tau_c]\}$, which reduces to Gaussian (exponential) forms for $\tau_C \to \infty$ ($\tau_C \to 0$). The x-averaged $P_\mu A(\tilde{x})$ resulting from fits to Eq.(3) using the Kubo-Tomita form and its Gaussian limit for G(t) are shown in Fig. 3. We conservatively adopt the smaller $P_\mu A(\tilde{x})$ fitted with the Gaussian form.

The second run Cu target data exhibits significantly (4.7σ) smaller $P_\mu A(\tilde{x})$ than the other metal target data. Muon range-straggling calculations show that the 160 mg/cm^2 Cu target was too thin to stop the μ^+ well within the target, while the 220 mg/cm^2 Cu target, composed of two foils, suffered from μ^+ stopping between the foils. (In the first run the μ^+ stopped 0.5 rms straggling lengths deeper in the second foil due to less upstream material). We base our result on the other ten statistically consistent (χ^2=7.7) metal target data sets in Fig. 3. The target-averaged $P_\mu A(\tilde{x})$ for each x bin are shown in Fig. 4, the line being a fit to Eq. (2) using the world average values[7] of δ and ρ. The endpoint amplitude $P_\mu A(0)=\xi P_\mu \delta/\rho$ is thereby determined with a statistical error of ± 0.0016.

Corrections totaling +0.0013±0.0006 are applied to the fitted $\xi P_\mu \delta/\rho$ for any incomplete nulling of B_L, and for μ^+ depolarization by Coulomb scattering upstream of the target and e^+ scattering in the target evaluated by Monte Carlo studies. Table 1 summarizes the major systematic errors, which add in quadrature to ±0.0016. No correction is made for unknown sources of μ^+ depolarization in the stopping process. Since such effects, or any neglected background, can only decrease the apparent result we quote the limit $\xi P_\mu \delta/\rho > 0.9941$ (90% confidence). Our conservative use of the Gaussian spin relaxation form further strengthens this limit. The result implies $M(W_2) > 350$ GeV for any mixing angle ζ; $M(W_2) > 415$ GeV for $\zeta=0$; and $|\zeta| < 0.054$ for infinite W_2 mass.

The good agreement between the present μSR result and the previous endpoint rate analysis result[2] ($\xi P_\mu \delta/\rho > 0.9959$), despite differences in the major sources of possible systematic error, reinforces our confidence in each of them. Combining the two results sets the 90% confidence limits $\xi P_\mu \delta/\rho > 0.9969$; $M(W_2) > 410$ GeV for any ζ; $M(W_2) > 485$GeV for $\zeta = 0$, and $|\zeta| < 0.039$ for infinite W_2 mass.

This research was supported in part by the U.S. Department of Energy through Contracts No. DE-AC03-76SF00098 and AC02-ER02289.

TABLE 1.

Major sources of systematic error and their estimated contributions

Source of Systematic Error	Error
Coulomb scattering of μ^+	±0.0004
Coulomb scattering of e^+	±0.0004
Incomplete nulling of B_L	±0.0002
Definition of x=1	±0.0004
Momentum scale calibration	±0.0010
World average δ, ρ values	±0.0009
Reconstruction of θ_μ and θ_e	±0.0004
Energy-loss straggling of e^+	±0.0003
Fitted μ^+ mean life τ_μ	±0.0003

References

(a) Present address: Department of Physics, University of Colorado, Boulder, Colorado 80309

(b) Deceased

1 J.C. Pati and A. Salam, Phys. Rev. Lett. 31, 661 (1973), and Phys. Rev. D10, 275 (1974); R.N. Mohapatra and J.C. Pati, Phys. Rev. D 11, 566, 2588 (1975).

2 J. Carr et al., Phys. Rev. Lett. 51, 627 (1983) also refer to other limits on right-handed currents.

3 F. Scheck, Phys. Lett. 44C, 187 (1978); A.M. Sachs and A. Sirlin, in Muon Physics, edited by V. Hughes and C.S. Wu (Adademic, New York, 1975), Vol. 2, p. 50.

4 M.A.B. Bég et al., Phys. Rev. Lett. 38, 1252 (1977).

5 C.J. Oram et al., Nucl. Instrum. Methods 179, 95 (1981).

6 R. Kubo and K. Tomita, J. Phys. Soc. Japan 9, 888 (1954); A. Abragam, The Principles of Nuclear Magnetism (Oxford University Press, 1961), p. 439.

7 We used the world average values ρ=0.7517±0.0026, δ=0.7551±0.0085 quoted in Review of Particle Properties, Phys. Lett. 111B (1982), together with our preliminary new result δ=0.748±0.005 quoted in B. Balke et al., Lawrence Berkeley Laboratory Report No. LBL-18320, yielding the combined value δ=0.750±0.004.

Figure Captions

FIG 1. Data from the second of three running periods, constituting 73% of the total μSR data, with (a) 70-G, and (b) 110-G transverse fields. The exponential decay with μ^+ lifetime has been factored out.

FIG 2. Values of $P_\mu A(\tilde{x})G(t)$ for each μ^+ spin precession cycle with B_T = 70-G (circles) or 110-G (triangles). The curves assume Gaussian μ^+ spin relaxation functions, $G(t)=\exp(-\sigma^2 t^2)$.

FIG 3. Values of $P_\mu A(\tilde{x})$ averaged over x bins, for (a) Gaussian and (b) Kubo-Tomita forms of G(t). The targets are Al (circles) 150 mg/cm^2 and 280 mg/cm^2 (marked "t"), Cu (squares) 160 mg/cm^2 and 220 mg/cm^2 (marked "t"), Ag (triangles) 270 mg/cm^2, and Au (inverted triangles) 240 mg/cm^2, with B_T = 110G (open symbols) or 70G (filled symbols). The Run 2 Cu target data are inconsistent with the average of the other data (solid line).

FIG 4. Values of $P_\mu A(\tilde{x})$ in each x bin for metal targets, excluding run 2 Cu. Error bars are statistical errors added in quadrature to the possible systematic error from the spectrometer momentum calibration. The line is a fit to Eq. 2 using world average values of δ and ρ.

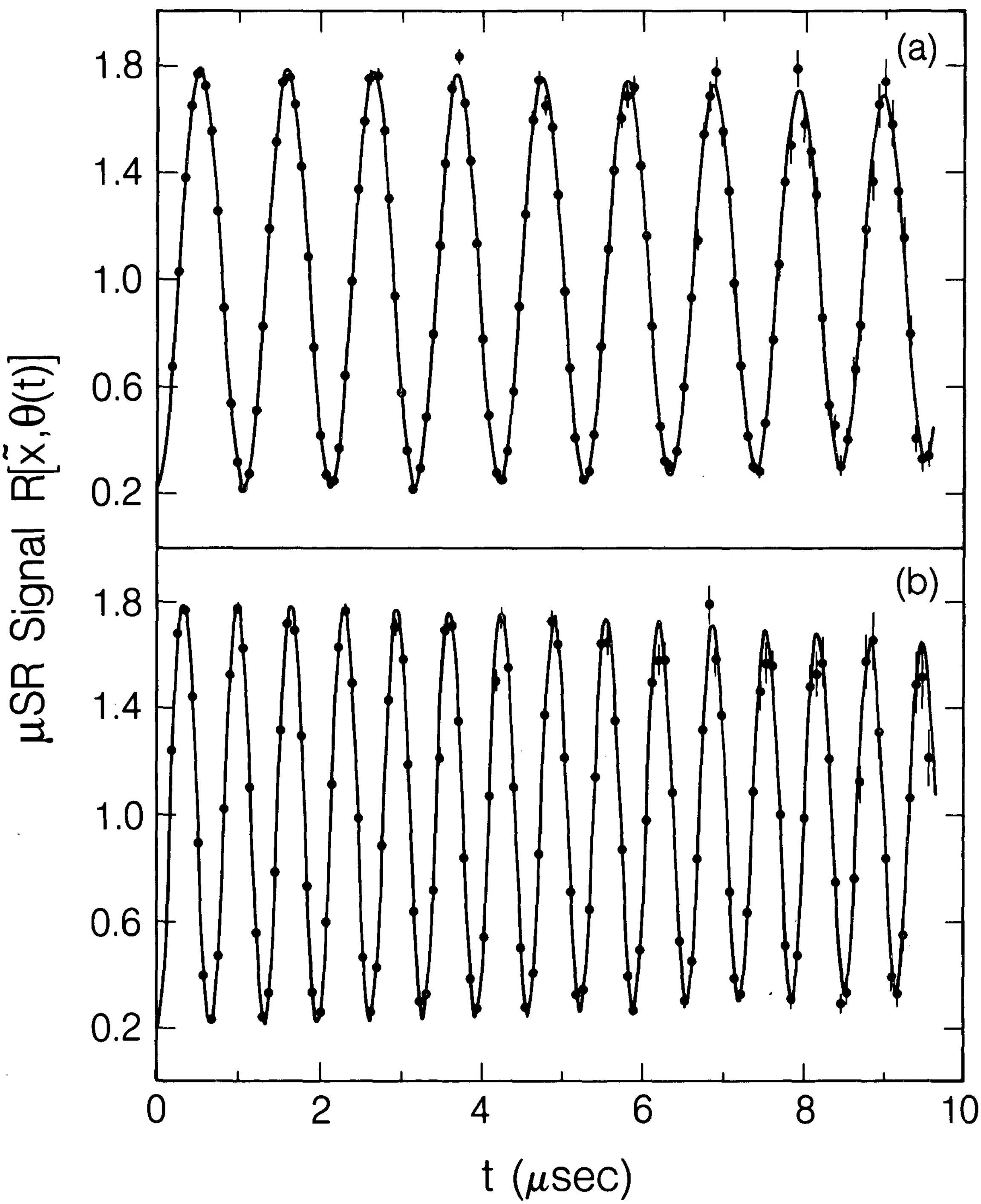

XBL 8412-6004

FIG. 1

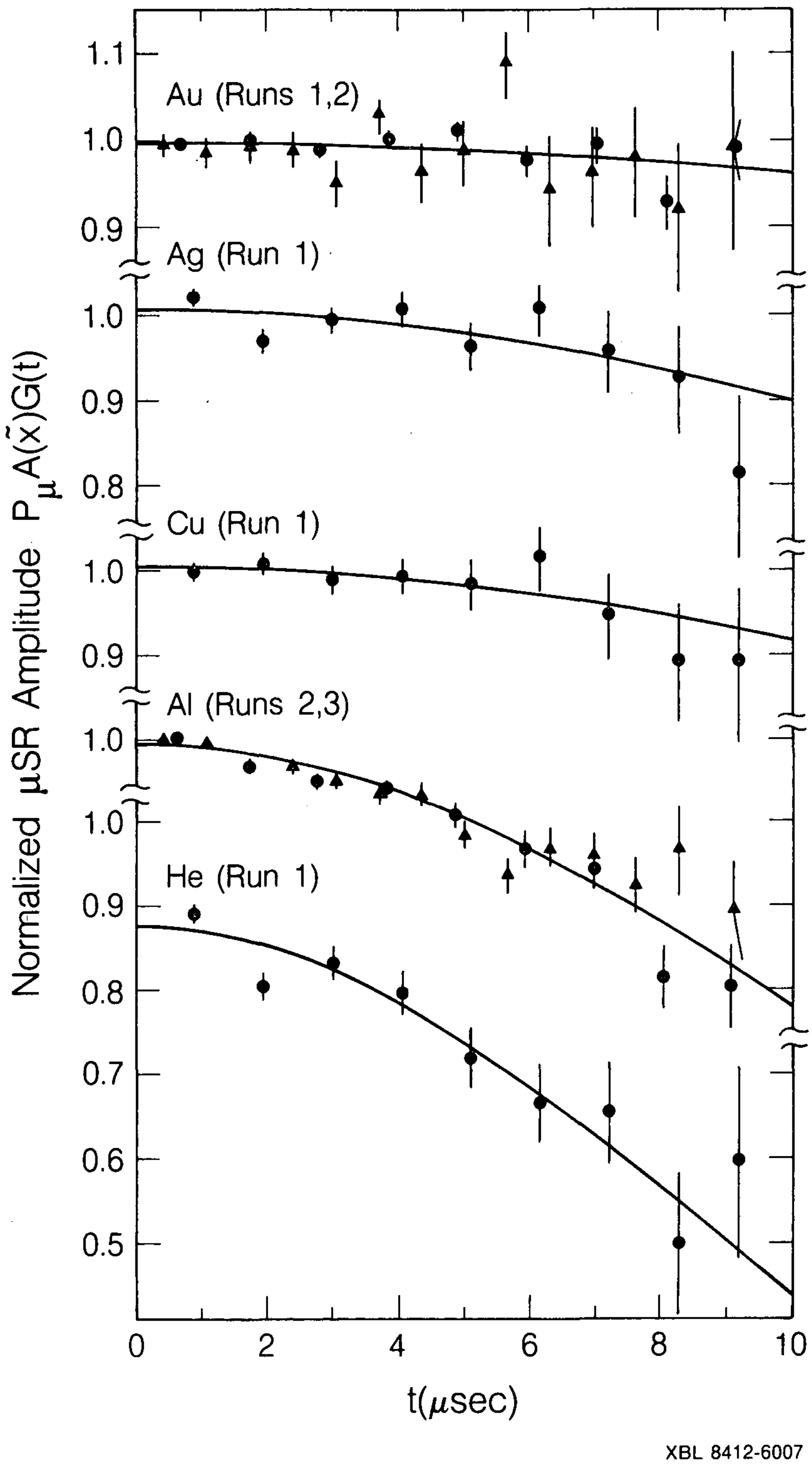

Au (Runs 1,2)
Ag (Run 1)
Cu (Run 1)
Al (Runs 2,3)
He (Run 1)
Normalized μSR Amplitude $P_\mu A(\tilde{x})G(t)$
1.1
1.0
0.9
0.8
0.7
0.6
0.5
0
2
4
6
8
10
t(μsec)
XBL 8412-6007

FIG. 2

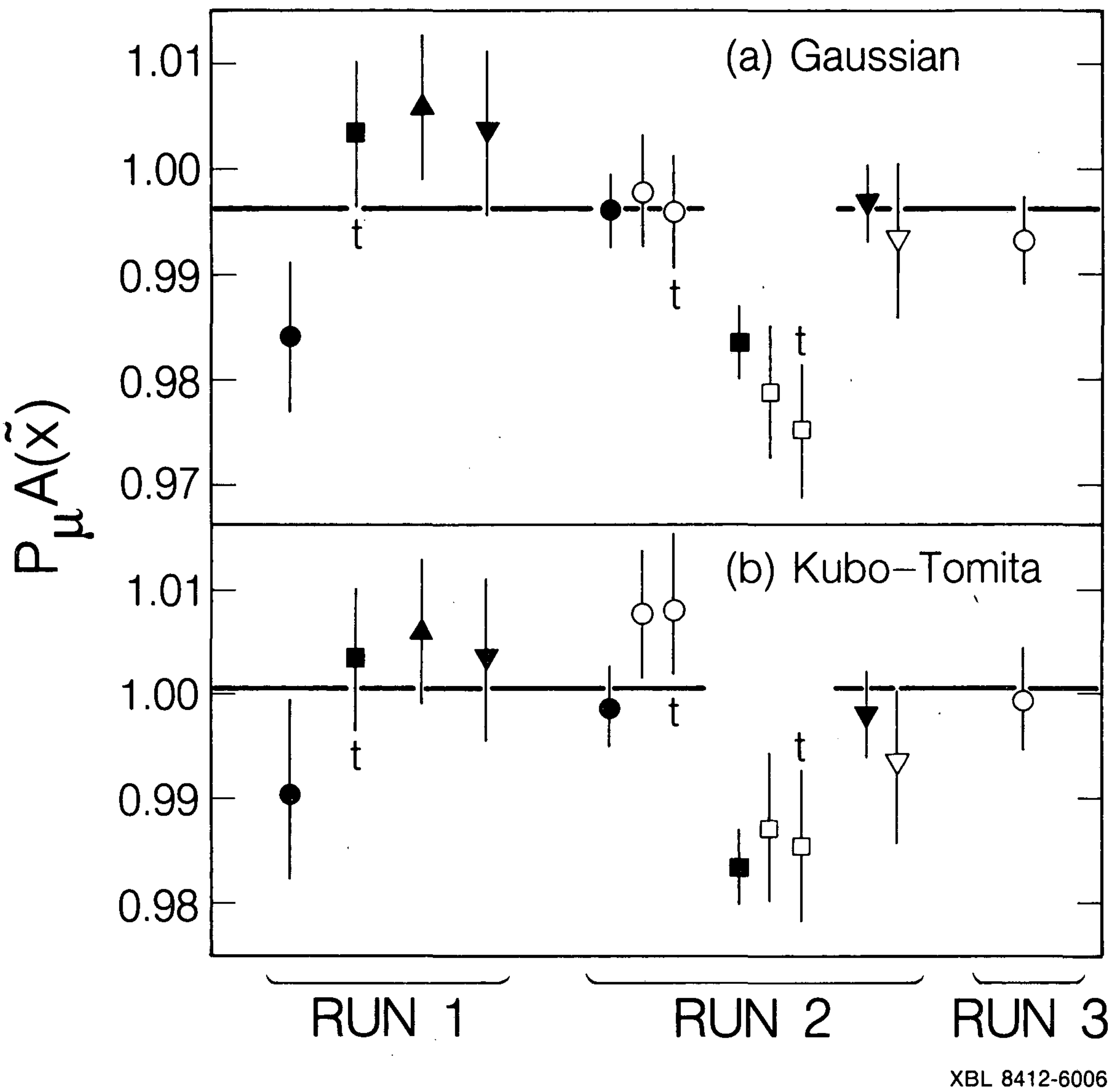

(a) Gaussian
(b) Kubo–Tomita
1.01
1.00
0.99
0.98
0.97
$P_\mu A(\tilde{x})$
t
RUN 1
RUN 2
RUN 3
XBL 8412-6006

FIG. 3

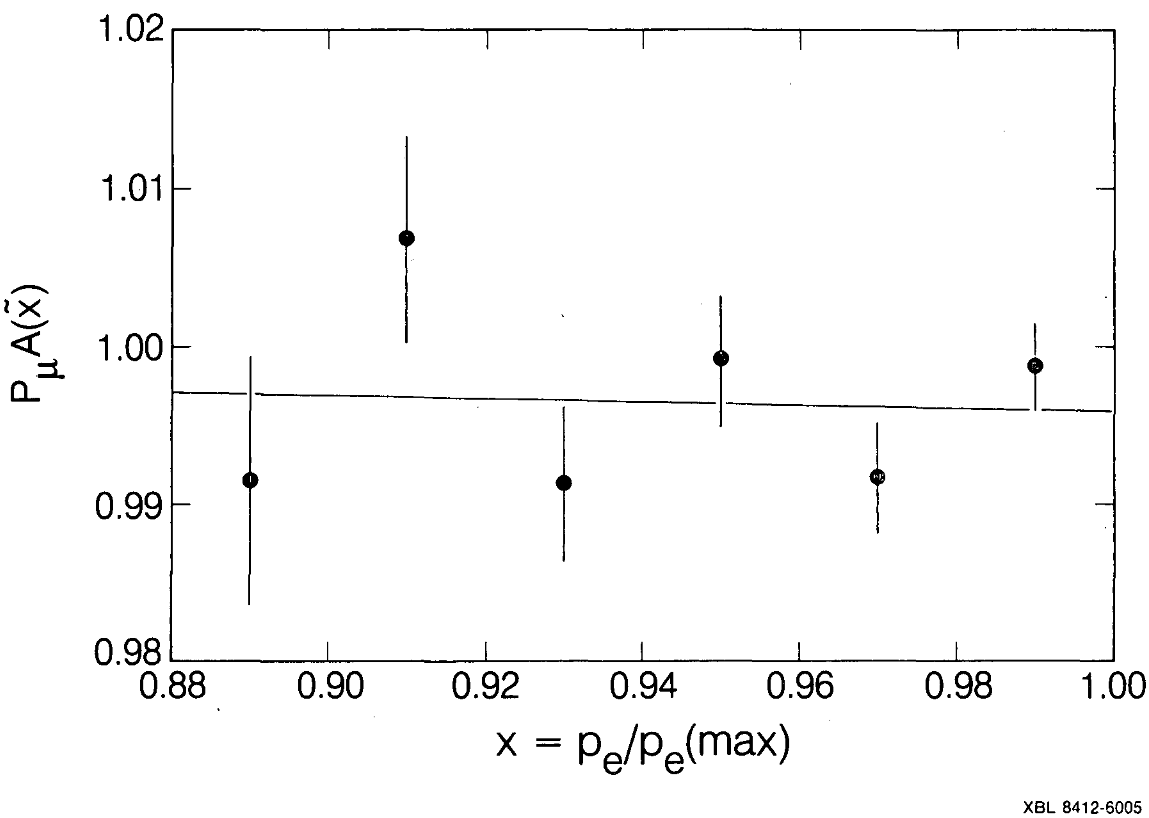
1.02
1.01
1.00
0.99
0.98
$P_\mu A(\tilde{x})$
0.88
0.90
0.92
0.94
0.96
0.98
1.00
$x = p_e/p_e(max)$
XBL 8412-6005

FIG. 4

TECHNICAL INFORMATION DEPARTMENT
LAWRENCE BERKELEY LABORATORY
UNIVERSITY OF CALIFORNIA
BERKELEY, CALIFORNIA 94720